Light-Emitting Diodes Based on All-Quantum-Dot Multilayer Films and the Influence of Various Hole-Transporting Layers on the Performance *

Hui-Li Yin(尹慧丽)[1,2], Su-Ling Zhao(赵谡玲)[1,2]**, Zheng Xu(徐征)[1,2], Li-Zhi Sun(孙立志)[1,2]

[1]*Institute of Optoelectronic Technology, Beijing Jiaotong University, Beijing 100044*
[2]*Key Laboratory of Luminescence and Optical Information (Ministry of Education), Beijing Jiaotong University, Beijing 100044*

(Received 5 December 2015)

We present a systematic analysis of the exciton-recombination zone within all-quantum-dot (QD) multilayer films using sensing QD layers in QD-based light-emitting diodes (QLEDs), and demonstrate the all-QD multilayer films with different sequences of layers prepared by inserting a sensing blue QD layer denoted as B at various positions within four red QD multilayers denoted as R. We also use different hole transporting layers (PVK, CBP as well as poly-TPD) to prevent the formation of leakage current and to improve the luminance. The results show that the total EL emission is mostly at the fourth (60%) and fifth (40%) QD monolayers, adjacent to ITO. This presents both decreasing current density and increasing brightness with different hole transporting layers, thus resulting in more efficient performance.

PACS: 73.21.La, 71.35.Cc, 73.50.Gr DOI: 10.1088/0256-307X/33/3/037301

Quantum-dot light emitting diodes (QLEDs) exhibit several advantages such as (i) the narrow emission line width (the full width half maximum about 30 nm compared with that of 60–80 nm of organic light emitting diodes (OLEDs)),[1,2] (ii) the easier tunability of color emission in the whole visible regime by tuning the particle size and shape,[3,4] and (iii) the significantly lower emitter cost for QLEDs compared with organic phosphorescent emitters.[5–8] According to those characteristics, QLEDs have been regarded as a significant candidate for the next-generation solid-state lighting and displays. Since the first demonstration two decades ago,[9] some key device parameters including the external quantum efficiency, brightness, and current efficiency of QLEDs have improved significantly as a result of the optimization of the device architecture and advancement of the fabrication techniques,[10–12] the choices of proper materials for charge injection and transportation[13,14] and the structural variation of the quantum dots (QDs) themselves.[15–17] Recent reports have demonstrated that some features of QLEDs can be comparable, or even superior to other high-performance polymer/small-molecule OLEDs,[18,19] further proving their competence for an important role in optoelectronic area. However, in QLEDs, because most quantum dots are in n-type materials, the unbalanced carrier may lead to a low current efficiency in devices. Although we have seen innovations and creativity in QLEDs, there have been few studies on light-emitting diodes based on all-quantum-dot multilayer films so far.

It is well-known that the p-type conductivity and hole injection barriers of the organic hole transport layer are crucial to the efficiency of QLEDs and OLEDs.[20] Hence, considerable effort has been taken to doping the organic layer(4,4'-N,N'-dicarbazole-biphenyl (CBP), poly (N-vinylcarbazole) (PVK) and poly (N,N'-bis(4-butylphenyl)-N,N'-bis(phenyl)-benzidine) (poly TPD)) in this work, as the intermediate hole transport layer (HTL) to balance the charge injection for high efficiency QLEDs with high work function.

In this Letter, the device structure of ITO/poly (ethylenedioxythiophene): polystyrene sulphonate (PEDOT : PSS) (3000r, 40 nm)/5QDs(PFN(PFN-P1 (Poly(9,9-bis(3'-(N,N-dimethyl)-propyl-2,7-fluorene)-alt-2,7-(9,9-dioctylfluorene))) between QD layer/LiF (0.5 nm)/Al (100 nm) was adopted for the QLEDs as shown in Fig. 1. All-QD multilayer films with different sequences of layers were prepared by inserting the sensing blue QD layer denoted as B at various positions within four red QD multilayers denoted as R. The devices are denoted as R4B1, R3B1R1, R2B1R2, R1B1R3 and B1R4, respectively, depending on the sequences of QD layers from the bottom closed to the anode side. PEDOT: PSS was used as the buffer layer on the anode mainly to increase the anode work

*Supported by the National High Technology Research and Development Program of China under Grant No 2013AA032205, the National Natural Science Foundation of China under Grant Nos 11474018, 51272022 and 61575019, the Specialized Research Fund for the Doctoral Program of Higher Education of China under Grant Nos 20120009130005 and 20130009130001, and the Technological Development Contract under Grant No HETONG-150188-04E008.

**Corresponding author. Email: slzhao@bjtu.edu.cn

© 2016 Chinese Physical Society and IOP Publishing Ltd

function from 4.7 eV (ITO) to 5.2 eV and to reduce the surface roughness of the anode to obtain stable and pin-hole-free electrical conduction across the device. The QD multilayer films were fabricated layer by layer through the sequential deposition of a concentration of 5 mg/ml QDs onto the substrates. The CdSSe-CdS core-shell red and blue quantum dots (ten monolayers of CdS shell) with phase-pure zinc blend structure were synthesized at Nanjing Technology Corporation. To obtain homogeneous and uniform QD multilayer films with well-defined internal structures, a spin-assisted assembly method was employed to flatten each layer by air-shear force and centrifugal force during the spinning process. The maximum coverage of each QD layer was obtained by a barrier layer of PFN spin-coated between each QD layer to prevent the dissolving of the front QDs layer by coating the next QDs layer. The barrier layer PFN was chosen due to the fact that not only is it immiscible with QD oil solvent to make sure the successful deposition of each layer, but also it emits almost no electroluminescence, which guarantees the color purity of the EL spectra of the QD multilayer films. The prepared PFN was diluted with the concentrated solution from 0.2% to 0.02%, and we used a thermal annealing process at 70℃ after each layer's spin coating.

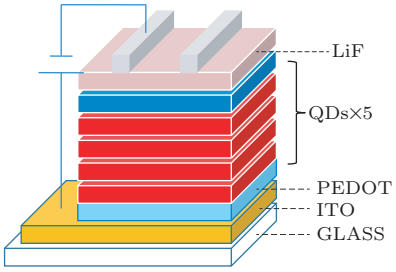

Fig. 1. Device structure.

Firstly, to confirm the phase of QD films, we measured the AFM characterizations of different numbers (n = 1, 3 and 5) of QD layers in the device configuration. For each layer, the height image, the pseudo-three-dimensional image and the phase image are shown in Fig. 2. It shows that the surface is filled with QD nanocrystals and the roughness of surface of five QD layers is rougher than that of three and one layers, which indicate the successful deposition of each layer. Extensive AFM measurements show that the rms roughness for the quantum dot layers are 1.86 nm (n = 1), 1.97 nm (n = 3), 2.04 nm (n = 5), respectively. The prepared multilayer films possess a flat and uniform surface morphology, while minor defects still existed, i.e., small vacancies between adjacent QDs or partial aggregates of QDs originating from the spherical geometry of the QDs and imperfections in the QD layering.

Moreover, the exciton-recombination zone within the QLEDs comprising five QD layers was investigated by monitoring the EL spectra changing with the introduction of the sensing blue QD layer at different locations (Fig. 3). The insets show the emission layer structure of each QLED (pixel size of $3 \times 3\,\mathrm{mm}^2$).

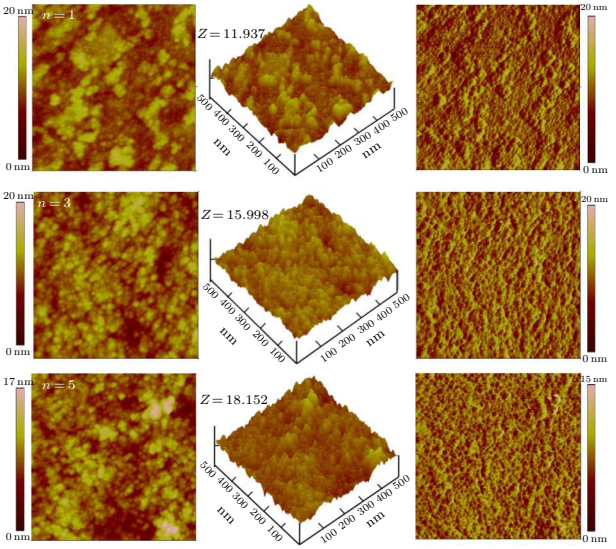

Fig. 2. AFM characterizations of different numbers (n = 1, 3 and 5) of QD layers.

As shown in Fig. 3, the devices with the emission layer of R4B1, R3B1R1, or R2B1R2 present the EL emission around a peak of 632 nm when the blue QD layer locates at the first, the second and the third layers from the side of cathode Al. When the sensing blue QD layer nears the ITO side, i.e., at the fourth and the fifth QD layers, the corresponding devices show the EL with two peaks at 452 nm and 632 nm, which originate from the emission of the blue QDs layer and the red QDs layer, respectively. In Figs. 3(d) and 3(e), approximately 60% and 40% of the total EL emission is blue coming from the fourth blue QD layer and the fifth QD monolayer, respectively. It is concluded that the excitons recombine mostly at the fourth (60%) and the fifth (40%) QD monolayer, which closes to the ITO side. The results are consistent with the evidence presented in previous reports regarding the quantum dot's excellent electron transport ability. Therefore, when the sensing blue QDs are near the ITO side, the blue EL will be detected. However, when the blue QDs are near the Al side, there is only red EL detected. In addition, it is noteworthy that no significant energy transfer from the blue QDs with the higher band gap to those red QDs with the lower band gap within QD multilayer films was observed in the EL spectra, which stands in contrast with previously reported results observed in the PL spectra of QD multilayer films.[21] This is considered to originate from the structure and composition of these QDs, since CdSSe/ZnS nanocrys-

tals are CdSSe cores coated with multiple layers of the semiconductor ZnS with a large band gap. The ZnS coating helps to protect and stabilize the unique optical properties of the CdSSe cores from the effect of environment emission.

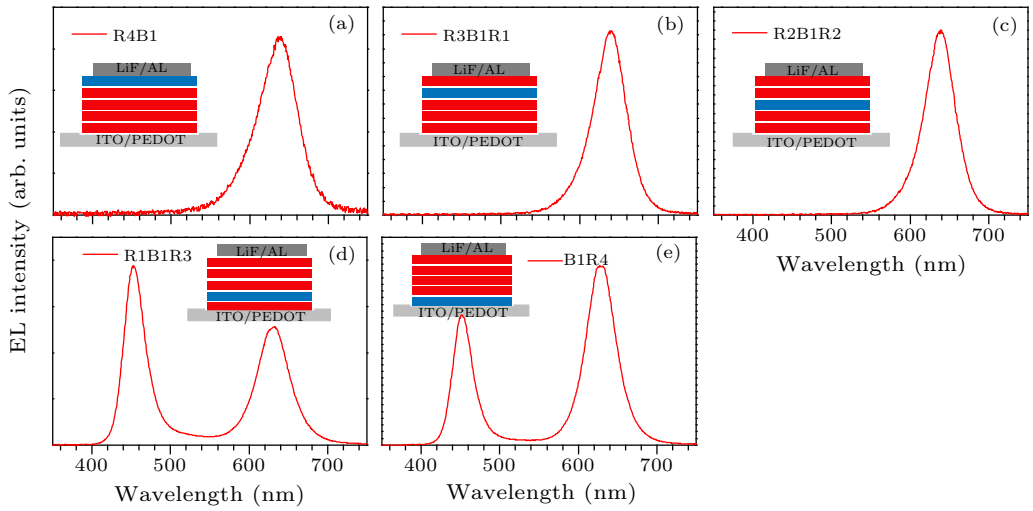

Fig. 3. Device structures and corresponding EL spectra (at 11 V) of QLEDs comprising sensing a blue QD layer at different positions within red QD multilayer films.

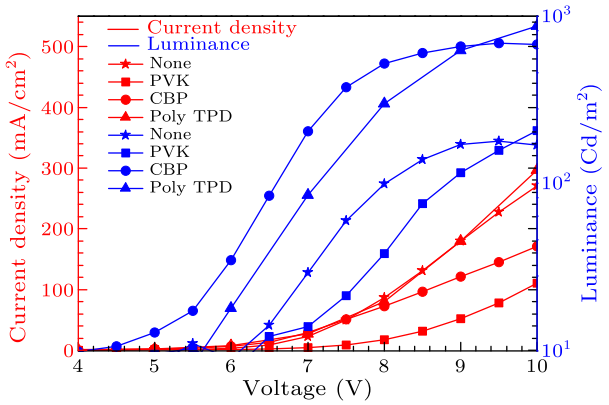

Fig. 4. Current density-voltage-luminance (I–V–L) characteristics of QLEDs with different HTLs prior to QD layers. The QLEDs comprising sensing the blue QD layer at the first layer adjacent to AL within red QD multilayer films (device denoted as R4B1) and a series of devices with and without different hole transporting layers (PVK, CBP and poly TPD) of device R4B1 are constructed.

Finally, the I–V–L characteristics of QLEDs based on the emission layer of R4B1 with different HTLs were carried out to improve the device performance (Fig. 4). The device structure is ITO/PEDOT: PSS/HTL/ R4B1/LiF/Al. It can be seen that the current density and luminance of all devices increase with the augmentation of driving voltage, and in the range of high electric field, the current density and luminance have a relationship of exponential function with the bias voltage, which is in good accordance with the typical diode characteristics. However, the main problem associated with such devices is the unbalanced charge transporting ability attributed to the fast electron transfer ability of QDs and the thin barrier film PFN, which results in a large leakage current. From Fig. 4 we can see that the current density of a device without HTL is ~250 mA/cm^2 and the brightness is 150 Cd/m^2 at 10 V merely. To decrease the leakage current to balance the charge and to enhance the luminance, the devices with similar emission layer sequences while having different HTLs were fabricated under the same conditions. PVK, CBP as well as poly TPD were used. As the hole injection barrier decreases, the leakage current density reduces at a given voltage, which indicates more balanced electron and hole charge densities within the emission layer.

As shown in Fig. 4, the QLEDs show a different turn-on voltage with different HTLs. Meanwhile, in devices with CBP as HTL at 10 V, we can see both decreasing current density (meaning effective prevention of the leakage current) and increasing brightness, thus resulting in more efficient performance. However, there is a noticeable decrease in the current density in devices where PVK is used but does not have much improvement at luminance. The barrier height difference among these HTLs does not differ much (TPD: 2.4, CBP: 2.5, PVK: 2.3), while the change in the current density is far more drastic. It is indicated that the barrier height for the charge injection cannot describe the significant decrease of the current density of devices with PVK as HTL. Alternatively, we suspect that this is in part due to the much lower charge mobility of PVK compared with the poly TPD. It is well known that PVK is an amorphous polymer with a low hole mobility, while the electron mobility of QDs has a high electron mobility, the holes from HTL in PVK are not able to balance the electrons from QDs

as electron transporting layers (ETL).

In conclusion, we have reported high-brightness QLEDs based on all-QD multilayer films prepared by a barrier layer of PFN spin-coated between each QD layer to overcome dissolution of each QD layer. Optimal QD coverage is found to be five monolayers for the best uniform film-forming performance. The exciton recombination zone is investigated by monitoring the EL spectral change with the introduction of a blue sensing layer within the all-QD multilayer films. The total EL emission is mostly at the fourth (60%) and the fifth (40%) QD monolayers, which is adjacent to ITO. The first, second and third layers play not only the part of emitting layer (EML), but also ETL in those devices. Furthermore, the devices with the same layer sequence but having different HTLs (CBP, PVK, poly TPD) are fabricated to decrease the leakage current, to balance the charge and to enhance the luminance. The results show that the current density is decreased and the brightness is increased when HTL is poly TPD. The barrier height for charge injection cannot be a contributor to the significant decrease in current density, while the hole mobility might be a possible influencing factor. This work proves a way for the fabrication of composite hole-transporting layers and provides solutions to enhance the luminous characteristics of OLEDs.

References

[1] Shirasaki Y, Supran G J, Bawendi M G and Bulovic V 2012 *Nat. Photon.* **7** 13

[2] Bae W K, Kwak J, Lim J, Lee D, Nam M K, Char K, Lee C and Lee S 2010 *Nano Lett.* **10** 2368

[3] Yang X, Zhao D, Leck K S, Tan S T, Tang Y X, Zhao J, Demir H V and Sun X W 2012 *Adv. Mater.* **24** 4180

[4] Anikeeva P O, Halpert J E, Bawendi M G and Bulovic V 2009 *Nano Lett.* **9** 2532

[5] Qian L, Zheng Y, Xue J and Holloway P H 2011 *Nat. Photon.* **5** 543

[6] Schreuder M A, Xiao K, Ivanov I N, Weiss S M and Rosenthal S J 2010 *Nano Lett.* **10** 573

[7] Tan Z, Zhang F, Zhu T, Xu J, Wang A Y, Dixon J D, Li L, Zhang Q and Mohney S E 2007 *Nano Lett.* **7** 3803

[8] Tan Z, Zhang Y, Xie C, Su H, Liu J, Zhang C, Dellas N, Mohney S E, Wang Y, Wang J and Xu J 2011 *Adv. Mater.* **23** 3553

[9] Colvin V, Schlamp M and Alivisatos A 1994 *Nature* **370** 354

[10] Kim L, Anikeeva P O, Coe-Sullivan S A, Steckel J S, Bawendi M G and Bulovic V 2008 *Nano Lett.* **8** 4513

[11] Wood V, Panzer M, Halpert J, Caruge J M, Bawendi M and Bulovic V 2009 *ACS Nano* **3** 3581

[12] Zhao J, Bardecker J A, Munro A M, Liu M S, Niu Y, Ding I K, Luo J, Chen B, Jen A K Y and Ginger D S 2006 *Nano Lett.* **6** 463

[13] Caruge J M, Halpert J E, Bulovic V and Bawendi M G 2006 *Nano Lett.* **6** 2991

[14] Caruge J, Halpert J, Wood V, Bulovic V and Bawendi M2008 *Nat. Photon.* **2** 247

[15] Anikeeva P O, Halpert J E, Bawendi M G and Bulovic V 2007 *Nano Lett.* **7** 2196

[16] Schlamp M, Peng X and Alivisatos A 1997 *Appl. Phys.* **82** 5837

[17] Li J J, Wang Y A, Guo W, Keay J C, Mishima T D, Johnson M B and Peng X 2003 *J. Am. Chem. Soc.* **125** 12567

[18] Dai X, Zhang Z, Jin Y, Niu Y, Cao H, Liang X, Chen L, Wang J and Peng X 2014 *Nature* **515** 96

[19] Mashford B S, Stevenson M, Popovic Z, Hamilton C, Zhou Z Q, Breen C, Steckel J, Bulovic V, Bawendi M, Coe-Sullivan S and Kazlas P T 2013 *Nat. Photon.* **7** 407

[20] Kim T H, Cho K S, Lee E K, Lee S J, Chae J, Kim J W, Kim D H, Kwon J Y, Amaratunga G, Lee S Y, Choi B L, Kuk Y, Kim J M and Kim K 2011 *Nat. Photon.* **5** 176

[21] Franzl T, Klar T A, Schietinger S, Rogach A L and Feldmann J 2004 *Nano Lett.* **4** 1599